Follow us @BoneJointRes

Freely available online OPEN ACCESS

BJR

KNEE

Does tibial design modification improve implant stability for total knee arthroplasty? An experimental cadaver study

S. Jaeger,
M. Eissler,
M. Schwarze,
M. Schonhoff,
J. P. Kretzer,
R. G. Bitsch

From University of Heidelberg, Heidelberg, Germany

Aims

One of the main causes of tibial revision surgery for total knee arthroplasty is aseptic loosening. Therefore, stable fixation between the tibial component and the cement, and between the tibial component and the bone, is essential. A factor that could influence the implant stability is the implant design, with its different variations. In an existing implant system, the tibial component was modified by adding cement pockets. The aim of this experimental in vitro study was to investigate whether additional cement pockets on the underside of the tibial component could improve implant stability. The relative motion between implant and bone, the maximum pull-out force, the tibial cement mantle, and a possible path from the bone marrow to the metal-cement interface were determined.

Methods

A tibial component with (group S: Attune S+) and without (group A: Attune) additional cement pockets was implanted in 15 fresh-frozen human leg pairs. The relative motion was determined under dynamic loading (extension-flexion 20° to 50°, load-level 1,200 to 2,100 N) with subsequent determination of the maximum pull-out force. In addition, the cement mantle was analyzed radiologically for possible defects, the tibia base cement adhesion, and preoperative bone mineral density (BMD).

Results

The BMD showed no statistically significant difference between both groups. Group A showed for all load levels significantly higher maximum relative motion compared to group S for 20° and 50° flexion. Group S improved the maximum failure load significantly compared to group A without additional cement pockets. Group S showed a significantly increased cement adhesion compared to group A. The cement penetration and cement mantle defect analysis showed no significant differences between both groups.

Conclusion

From a biomechanical point of view, the additional cement pockets of the component have improved the fixation performance of the implant.

Cite this article: *Bone Joint Res* 2022;11(4):229–238.

Keywords: Attune, Attune S+, Cement debonding, Implant stability, Cement pockets

Article focus

- The aim of this experimental in vitro study was to investigate whether additional cement pockets on the underside of the tibial component could improve implant stability.

Key messages

- From a biomechanical point of view, this has further improved the fixation performance of the implant.

Correspondence should be sent to Sebastian Jaeger; email: sebastian.jaeger@med.uni-heidelberg.de

doi: 10.1302/2046-3758.114.BJR-2021-0169.R1

Bone Joint Res 2022;11(4):229–238.

Strengths and limitations

- The high degree of standardization allows direct conclusions regarding the implant design.
- However, the transferability of the experimental data to the patient should be confirmed by clinical studies.

Introduction

One of the most common causes of revision in total knee arthroplasty (TKA) is aseptic loosening,[1] with the overall number of cases expected to increase in the coming years.[2] A study of 21,000 evaluated tibial components found a correlation between early migration and late loosening, and showed that early increased relative motion could increase the risk of revision by up to 8%.[3] The reasons for loosening of prostheses with increased relative motion at the implant interfaces can be manifold. Parameters such as stem length, surface texture, geometry, size of rotation-stabilizing elements, stem cementation, and cement pockets are reported in the literature as parameters responsible for implant interface stability.[4-8] In vivo results for the tibial component of the Attune knee system showed early aseptic loosening with failure of the cement-implant interface.[4] The authors assumed missing cement pockets and fewer rotation-stabilizing components as a reason for prosthesis loosening. Revision surgeries were performed on average 19 months after primary implantation.[4] Cerquiglini et al[9] used retrieval analysis to investigate the cement attachment at the underside of the tibial component, and found that there was no evidence of cement attachment for the investigated Attune components. In contrast, the predecessor model, the P.F.C. Sigma, showed evidence of cement adhesion. According to Cerquiglini et al,[9] the differences in cement attachment could be related to the design differences of these implants, especially with regard to the cement pockets. Another clinical study by Staats et al[10] showed a significantly higher incidence of radiolucent lines after 12 months below the tibial Attune prosthesis (35.1%) compared to the predecessor P.F.C. Sigma (7.5%). Therefore, it is important to investigate whether the newer model of the tibial Attune component with the design modification of the additional cement pockets can actually improve implant fixation.

Regarding cement application, however, there is some disagreement about the best approach.[11-13] Refsum et al[14] showed that in six out of ten cases, cement application was performed with a cement gun, and in four cases by finger-packing technique. The question of cement application to the undersurface of the prosthesis with or without cementation of the stem is still controversial. In this case, the advantages of presumably improved stability, due to additional stem cementation, are in contrast to the disadvantage of increased bone loss in the case of revision.[8,15-18] The evidence is clearer in terms of the further cementing procedure, preferring an early cement application to the prosthesis and subsequently to the prepared bone bed for increased interface stability.[19-22] Contamination with blood or lipids must be avoided, as these lead to significant degradation of the bond between the prosthesis, cement, and bone.[23]

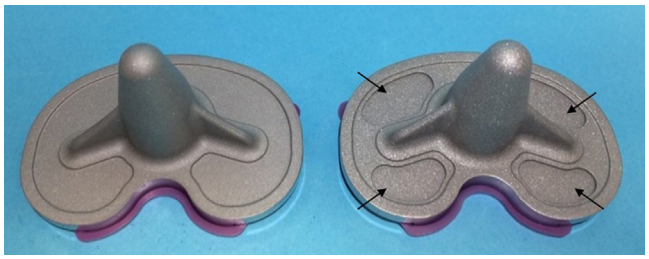

Fig. 1

Attune (left) and Attune S+ (right) tibia components with additional cement pockets.

The aim of this experimental in vitro study was therefore to investigate whether additional cement pockets on the underside of the tibial component could improve implant stability. As evaluation criteria, the relative motion between implant and bone, the maximum pull-out force, the tibial cement mantle, and a possible path from the bone marrow to the metal-cement interface were determined in human cadaver legs.

Methods

The following in vitro study using cadaveric specimens was structured into the following parts: the measurement of the relative motion under dynamic loading, and determination of the maximum pull-out force. Additionally, a radiological determination of bone mineral density (BMD) and 2D and 3D cement penetration analyses were conducted. The study received a positive vote from the local ethics committee (Ethics Committee Heidelberg). In 15 pairs of fresh frozen human legs, the Attune total knee arthroplasty was implanted by an experienced surgeon (RGB). The regular Attune and the newer Attune S+ tibial components (both DePuy Synthes (USA), both fixed-bearing) were implanted in a randomized fashion. The differences between the two tibia designs are additional cement pockets and a modified surface roughness of the under-surface of the Attune S+ component (Figure 1).

The specimens were randomly allocated – right and left knee – to group A (Attune) or group S (Attune S+), by means of a computer-generated list (Randlist 1.2; Datinf GmbH, Germany). The donor data showed a mean age of 68.3 years (standard deviation (SD) 11.5), a mean height of 174.4 cm (SD 10.9), a weight of 75.1 kg (SD 16.4), and a BMI of 24.6 kg/m^2 (SD 4.7).

Radiological examinations with determination of implant size. Franck et al[24] showed a high correlation between standard dual-energy X-ray absorptiometry (DXA) at the hip and various locations such as the limbs. Therefore, we measured BMD using DXA with standard hip parameters (Hologic QDR-2000, USA). This allowed us to compare

the two groups and to assess bone quality. Native radiographs in anteroposterior (AP) and lateral projection of all 30 knee joints were obtained preoperatively, as it is common clinical practice. This allowed determination of prosthesis size using the TraumaCad software (Voyant Health, Brainlab AG, Germany) and exclusion of pre-damage. The same prosthesis size was planned and implanted on the right and left side of each pair of legs. This resulted in the following tibial implant sizes: size 3 (n = 1), size 4 (n = 3), size 5 (n = 2), size 6 (n = 2), size 7 (n = 5), and size 8 (n = 2). Postoperative radiographs were used to verify the implantation result and to exclude any intraoperative fractures.

Cementing procedure. Prior to surgery, the human legs were thawed at room temperature. To standardize the experimental conditions and the surgical steps, all adjustments and resection measurements were documented and transferred to the contralateral side. Bone bed preparations and implantations were performed according to the prosthesis manufacturer's surgical instructions. For the preparation of the keel, two different keel impactors are available for the Attune Knee System. Both are intended for cemented implantation. One is the cement mantle prep keel punch, which we used in this study, and the other is the line-to-line keel punch. Prior to cementation, the cancellous bone was cleaned of lipid deposits, blood, and bone debris using the OptiLavage system (Zimmer Biomet, USA) and dried with a compress until immediate cement application. The implantation of the group A and group S prostheses was performed with a vacuum mixed high viscosity bone cement (Optipac 40 Refobacin Bone Cement R, Zimmer Biomet). A two-stage cementation technique was used in order to be able to ensure an early cementation with early full leg extension for cement curing and thus to create optimal conditions. The cement was applied using early cement timing for vacuum-mixed cement at a room temperature of 21.2°C (± 0.2°C). We applied the bone cement to the under-surface of the tibial component 80 seconds after the start of the mixing process. In the next step the cement was applied to the bone at 110 seconds using the cement gun. The impaction of the tibial component was performed 140 seconds after start of mixing. Immediately thereafter, excess cement was removed, the femoral trial component with associated inlay was inserted, and the leg was placed in extension position at 240 seconds after start of mixing, where the cement was allowed to harden. The leg was left in extension position for ten minutes after start of mixing to ensure complete cement-hardening. The corresponding femoral component was implanted afterwards. The amount of cement used in the right-left comparison was verified by checking the weight of the cement cartridge together with the removed cement.

Load simulation and determination of relative motion. Before starting dynamic loading to measure relative motion, the femur and tibia were separated, and the soft-tissues were removed. Subsequently, the specimens were cast in a mould using synthetic resin (Rencast FC 53, Huntsman Advanced Materials, Germany) in order to be able to integrate the specimens into the material testing machine. For the assessment of implant stability, a tibiofemoral contact force (axial force) was applied in a sinusoidal double peak. In addition, a second actuator was used to apply extension-flexion between 20° and 50 ° (Figures 2 and 3). The load maxima (maximum force) occurred at the time of extension and flexion, respectively,[25] using a servo-hydraulic testing machine (MTS 858 Mini Bionix II, MTS Systems Corporation, USA) (Figure 2). The load corresponds to the daily activity of climbing stairs.[26-28] Initially, a preload of 200 N was applied before cyclic loading was started. Subsequently, the force was applied for 1,000 cycles per load level (4,000 cycles in total). The load level increase was incremental by 300 N (1,200 N, 1,500 N, 1,800 N, 2,100 N) (Figure 3). The measurement of the relative motion between implant and bone was performed using optical, camera-based measurement techniques (PONTOS-GOM – Gesellschaft für Optische Messtechnik mbH, Braunschweig, Germany). Bone and implant markers were applied to the prosthesis and at the line of resection to record the 3D relative motions (Figure 2). The maximum relative movements were evaluated in relation to all three spatial axes, with normalization to the right tibia for maximum extension and flexion (20°, 50°).

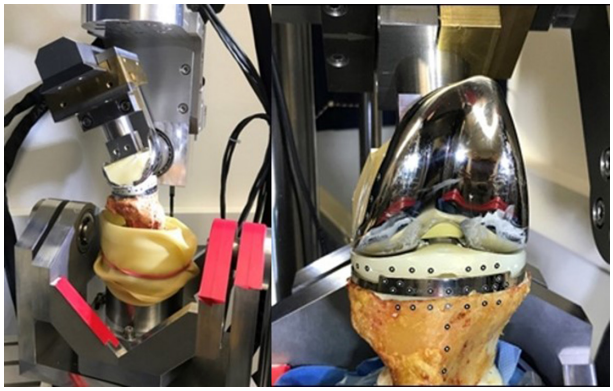

Fig. 2

Left: dynamic loading with extension and flexion. Right: applied bone and implant marker.

Maximum pull-out force and cement adhesion. Maximum failure load was determined using a pull-out test with a cross head speed increment of the material testing machine (MTS 858 Mini Bionix II, MTS Systems Corporation) of 2 mm/min (Figure 4) immediately after the cyclic loading. The maximum failure load was determined in the axial direction of the prosthesis stem.

After the pull-out test, the cement adhesion to the under surface of the prosthesis was also evaluated. For this purpose, the adherent cement quantity was evaluated in relation to the total area (without stem). To determine the cement adhesion, the underside of the prosthesis was digitized using a copy stand (Kaiser Fototechnik, Germany) with integrated Canon EOS 350D and a macro

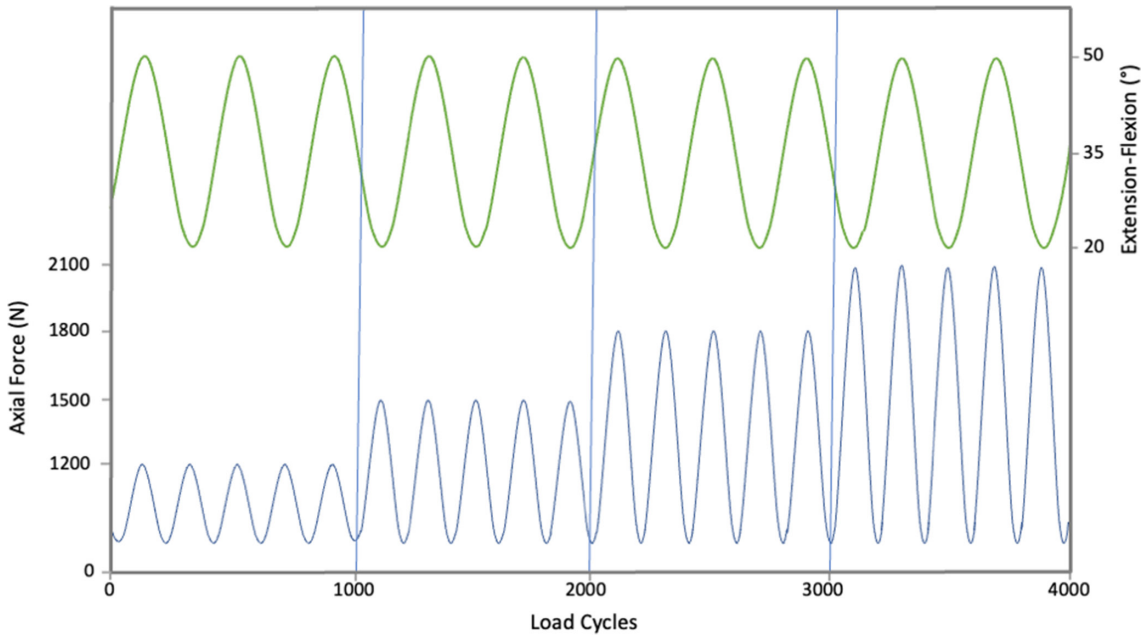

Fig. 3

The figure shows a schematic sinusoidal loading scenario with increasing load every 1,000 cycles. The synchronous extension-flexion is shown in the upper plot.

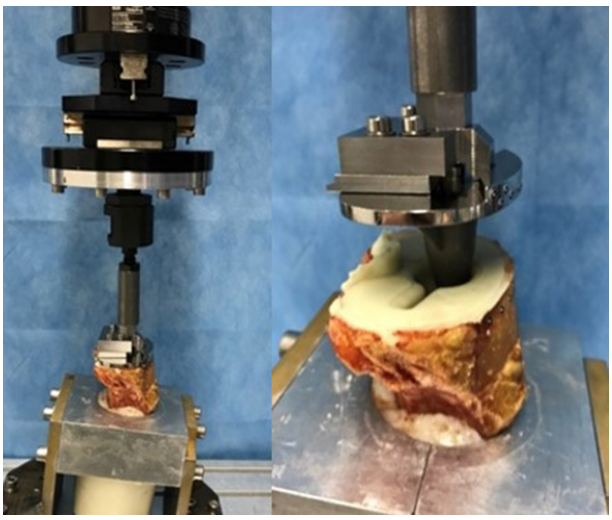

Fig. 4

Determination of the maximum failure load.

objective 1:2.8 DG (SIGMA, Germany). The assessment of the cement adhesion was performed using the software ImageJ 1.52 a (National Institutes of Health, USA).

Radiological cement analyses. Postoperative radiographs were used to measure the cement penetration area of each specimen in two planes. Using ImageJ 1.52, the area of cancellous bone penetrated by cement could be marked and measured (Figure 5).[29] Subsequently, the cement surface was calculated with the aid of a reference sphere. To be able to investigate possible cement defects of the cement mantle, and thus a possible direct connection from the fat marrow to the metal-cement interface, we obtained CT scans (SOMATOM Emotion; Siemens Healthcare, Germany) of the tibia specimens. The CT scans were performed, after determining the maximum failure load, with a slice thickness of 0.75 mm. Furthermore, we used the scans to measure the cement mantle defect area for the keel and stem of the two groups (Figure 6). In the first step, the cement was segmented from the CT scans using the ITK-SNAP software.[30] Subsequently, the cement defects were analyzed with the Geomagic Studio (Raindrop Geomagic, USA) program by measuring the defect area and calculating the percentage of the total embedding implant surface. A 0.9% saline solution mixed with blue pigment was injected into the medullary canal distally of the prosthesis tip (Figure 7) to check for cement defects with direct contact between the medullary canal and the under-surface of the implant. The only way for the fluid to escape from the medullary canal was through defective areas of the cement mantle. This could be proven by blue staining of the cement surface.

Statistical analysis. Prior to the start of the experimental study, a sample size calculation was performed using G*Power 3.1 (University Kiel, Germany),[31] based on the reported data by Schwarze et al.[32] Input parameters to compute the required sample size were tails: two, effect size d: 1.33, α err prob: 0.05 and power (1-β err prob): 0.95. This results in the output parameters sample size 16 for each group and an actual power of 0.95. A sample size of 15 paired fresh-frozen human legs were available for us. The data were evaluated descriptively using the arithmetic mean, SD, range, and 95% confidence intervals (CIs). Pre-analysis, the normal distribution of the data was evaluated using a Shapiro-Wilk test, and the homogeneity of variance was verified using Levene's test. We

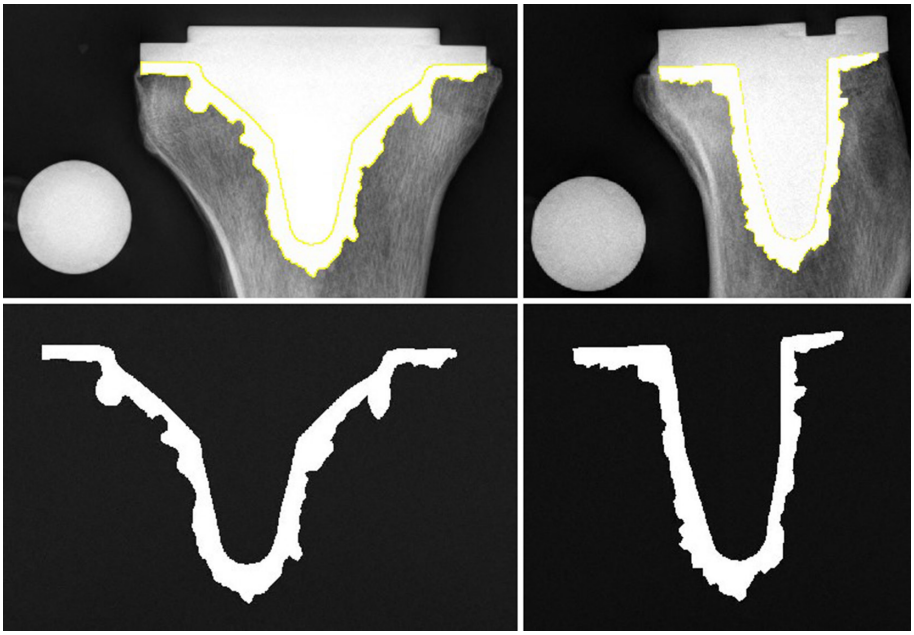

Fig. 5

2D X-ray analysis: cement penetration area in anteroposterior (left) and lateral direction (right).

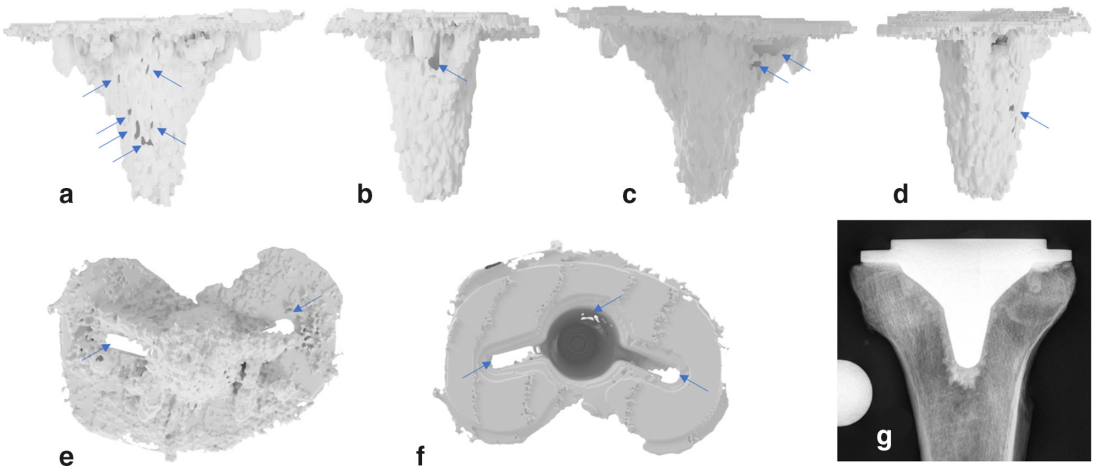

Fig. 6

CT scans with different views and blue arrows to mark the cement mantle defects. a) Anterior, b) lateral, c) posterior, d) medial, e) caudal, and f) cranial. g) The corresponding radiograph in anteroposterior projection without visible cement mantle defect.

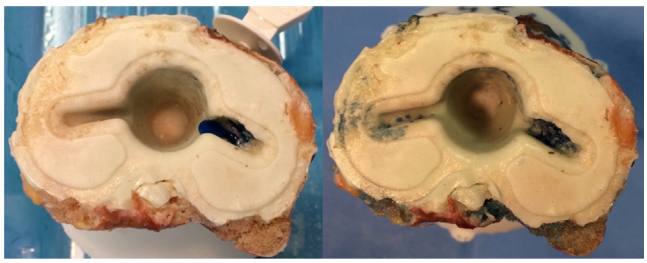

Fig. 7

For validation of the cement defects (using CT scans), and to check whether there was a direct connection between the medullary canal and the tibial component, 0.9% saline solution with blue pigments was injected into the medullary canal distally of the prosthesis tip.

conducted an independent-samples *t*-test to assess effects between both groups on the parameters BMD, maximum failure load, cement penetration, cement mantle defect, and relative motion within each load level. For the cement adhesion, we used the Mann-Whitney U test for normal distribution results. A repeated measures analysis of variance (RMANOVA) was conducted to investigate the dependent variable (relative motion) at four timepoints (load levels 1 to 4) for differences in means. Within-subject effects were examined for significant differences in the dependent variable over time. For the RMANOVA, a Greenhouse-Geisser adjustment was used to correct for violations of sphericity. All data were analyzed using SPSS 25 (IBM, USA) with a significance level of $p < 0.05$.

Table I. Maximum relative motion for 20° flexion and all investigated load levels.

Variable	Mean maximum relative motion, µm (SD)			
Load level, N	1,200	1,500	1,800	2,100
Group A	26.8 (3.1)	41.8 (5.5)	58.4 (4.8)	77.4 (5.5)
Group S	20.7 (2.4)	28.8 (2.5)	36.4 (2.2)	45.1 (2.4)

SD, standard deviation.

Table II. Maximum relative motion for 50° flexion and all investigated load levels.

Variable	Mean maximum relative motion, µm (SD)			
Load level, N	1,200	1,500	1,800	2,100
Group A	40.4 (5.0)	63.6 (6.6)	87.0 (5.6)	129.1 (13.2)
Group S	28.3 (3.8)	40.2 (2.3)	49.9 (2.3)	64.2 (4.1)

SD, standard deviation.

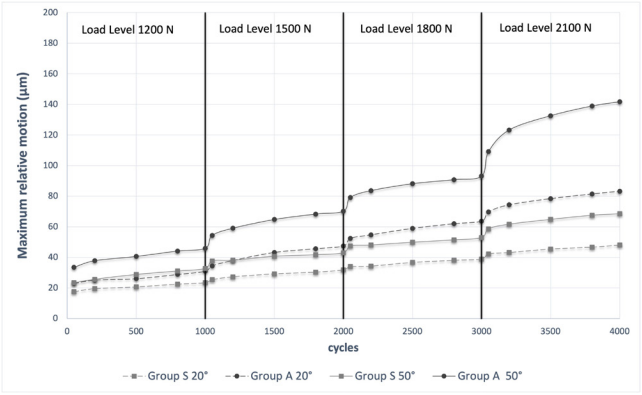

Fig. 8

Maximum relative motion of the design of group A and group S for an extension-flexion angle of 20° to 50°.

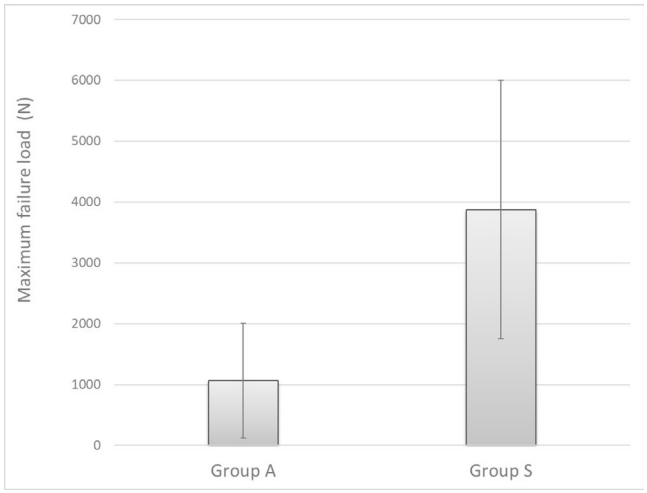

Fig. 9

Mean maximum failure load of the investigated prosthesis designs. The lines represent the standard deviations.

Results

One pair of legs was excluded from the relative motion analysis and maximum pull-out force due to a prosthesis loosening during the test preparations, and one pair of legs was excluded due to a fracture during the loading simulation.

Bone mineral density. No statistically significant difference was found in mean BMD between group A (0.882 g/cm² (SD 0.109)) and group S (0.891 g/cm² (SD 0.105)), (t(24) = -0.224; p = 0.824, independent-samples *t*-test (95% CI -0.096 to 0.077)).

Relative movement for 20° flexion. Relative motion showed statistically significant differences between load levels for 20° flexion (F (1.2, 9.8) = 3,093.9; p < 0.001) in the RMANOVA with a Greenhouse-Geisser correction.

When comparing the two prosthesis designs, the independent-samples *t*-test showed a significant difference in maximum relative motion at each of the four load levels (Table I, Figure 8). Group A showed consistently for 20° flexion a higher maximum relative motion compared to group S. At load level 1,200 N, there was a mean difference increase of 6.0 µm (95% CI 2.0 to 10.1) in maximum relative motion (t(8) = 3.4; p = 0.009). For load level 1,500 N, the mean difference increase was 12.9 µm (95% CI 6.7 to 19.1), (t(8) = 4.8, p = 0.001). For load level 1,800 N, the mean difference was 22.0 µm (95% CI 16.6 to 27.4), (t(8) = 9.4, p < 0.0o1). Finally, for load level 2,100 N, the mean difference was 32.3 µm (95% CI 26.1 to 38.5), (t(8) = 12.1, p < 0.001).

The RMANOVA showed that an increase of the load levels has a significant influence on the relative motion in 20° flexion (F (1.2, 9.8) = 3,093.9; p < 0.001), correction according to Greenhouse-Geisser.

Relative movement for 50° flexion. A statistically significant difference of relative motion between load levels for 50° flexion was seen in RMANOVA with Greenhouse-Geisser correction (F (1.1, 8.8) = 881.6; p < 0.001). Evaluation of the two tibial component designs using the independent-samples *t*-test showed a significant difference in maximum relative motion at each of the four load levels (Table II, Figure 8). Group A consistently showed a higher maximum relative motion compared to group S for 50° flexion. At load level 1,200 N, there was a mean difference increase of 12.1 µm (95% CI 5.6 to 18.6) in maximum relative motion (t(8) = 4.3; p = 0.003). For load level 1,500 N, the mean difference increase was 23.1 µm (95% CI 15.1 to 31.2), (t(5) = 7.4; p = 0.001). For load level 1,800 N, the mean difference was 37.1 µm (95% CI 30.8 to 43.4), (t(8) = 13.6; p < 0.001). Finally, for load level 2,100 N the mean difference was 64.9 µm (95% CI 48.7 to 81.1), (t(5) = 10.5; p < 0.001).

RMANOVA showed, for the main effect of the within-subject, that an increase of the load levels has a significant influence on the relative motion in 50° flexion (F (1.1, 8.8) = 881.6; p < 0.001), correction according to Greenhouse-Geisser.

Maximum failure load and cement adhesion. The independent-samples *t*-test showed a statistically significant difference in mean maximum failure load between

Fig. 10

Left: Group A (Attune). Centre: Group S (Attune S+) without adherent cement. Right: Group S with adherent cement.

group A (1,062.4 N (SD 942.6, 0.0 to 3,288.0)) and group S (3,876.7 N (SD 2,124.4, 1,372.0 to 7,426.0)) prosthesis designs ($t(18) = -4.5$, $p < 0.001$). There was a decreased maximum failure load of 2,814 N (95% CI -4,119.8 to -1,508.9) for the group A components. Group S, by contrast, showed a 265% increase in maximum failure load compared to group A (Figure 9). In nine cases, the Attune group showed values below 1,000 N for the maximum failure load, with one value at 0 N. Evaluation of percent cement adhesion to the under-surface of the tibial prosthesis was assessed with Mann-Whitney U test after pull-out. Group S showed significantly increased cement adhesion compared to group A ($U = 43$; $p = 0.034$). Group A showed a mean cement adhesion ratio of 0.3% (SD 0.9%). No cement remained on the underside of 12 group A prostheses, with a cement area of 3.3% in one (Figure 10). All group A prostheses showed a fat layer on the under-surface.

In group S, minimal cement residues remained in the cement pockets of nine components, and partial cement in three (Figure 10). One prosthesis under-surface was completely covered with cement and bone after pull-out. On average, a mean 12.3% (SD 27.3%) of the area in group S remained covered with cement. The group S tibial components also showed fat debris on the metal.

Cement penetration area and cement mantle defect. Mean cement penetration area for the anteroposterior (AP) direction was 426.7 mm^2 (SD 55.5) for group A and 464.8 mm^2 (SD 72.4) for group S. The independent-samples *t*-test showed that this difference was not statistically significant ($t(24) = -1.5$; $p = 0.146$ (95% CI -90.3 to -14.2)).

On the lateral radiographs, there was also no significant difference between group A (379.2 mm^2 (SD 58.9)) and group S (415.7 mm^2 (SD 85.1)), ($t(24) = -1.3$; $p = 0.215$, (95% CI -95.8 to 22.7)). The independent-samples *t*-test for the cement mantle defect in relation to the interface area between cement and metal showed no statistically significant difference between group A (2.3% (SD 2.3%)) and group S (3.4% (SD 2.2%)), ($t(24) = -1.3$; $p = 0.222$, (95% CI -2.9, to -0.7)).

Discussion

Aseptic loosening is still the most common cause of revision in TKA,[1,33] and can be influenced by a variety of different factors. These include factors that influence implant stability due to their design characteristics. These could be features such as the geometry and length of the prosthesis stem, and the presence of anti-rotation wings or cement pockets.[7,34,35] Furthermore, it has been shown that an adequate cementing technique with appropriate bone-cleansing can be crucial for cement penetration and thus for implant stability.[36,37]

The objectives of this study were to evaluate if there is a potential difference in relative motion between the Attune and Attune S+ tibia components, and their behaviour related to the maximum failure load under standardized test conditions. We also analyzed the tibial cement mantle defect, cement penetration area, and cement adhesion. Additionally, bone density was determined to ensure that there were no significant differences between both groups. The results of the 3D in vitro measurements of the relative motion between tibial component and bone were evaluated at 20° and 50° flexion. Group A showed for all four load levels significantly higher mean maximum relative motion compared to group S for 20° and 50° flexion. At the load level of 2,100 N, the group A tibial base showed values of 129.1 µm (SD 13.2) compared to 64.2 µm (SD 4.1) for group S. These were the highest values for both groups. For both investigated groups and flexion angles, the mean maximum relative motion showed a significant increase with increased load levels. The observed range of the maximum failure load showed values between 0 and 3,288 N for group A and 1,372 and 7,426 N for group S. The Attune S+ component, with its additional cement pockets, significantly improves the maximum failure load compared to the Attune without additional cement pockets. For group A, we set the value for the maximum failure load to 0 N, since the prosthesis loosening occurred before the relative motion was determined. When preparing the specimen for insertion of the polyethylene inlay to determine the relative motion under dynamic loading, we found that the tibial Attune component had already loosened. Therefore, we assessed the pull-out force as 0 N. A possible cause could be the combination of impaction and ligament tension force. The ligament tension force during cement hardening and the impaction force must exceed the radial press fit. Jaeger et al[38] found an increased radial press fit around the

tibial stem and keel, with growing radii of the rounded tibial edges and with decreasing cement mantle space around the implants. The Attune component showed a 2 mm radial press fit with maximum incomplete seating of 1.8 mm for the cement mantle instrumentation. The radial press fit effect as reported by Jaeger et al[38] could be enhanced in sclerotic bone. Evaluation of the post-operative radiographs showed no significant differences in the cement penetration area for the AP or the lateral radiographs between both investigated groups. The examination of the cement mantle showed no significant difference for the cement mantle defect related to the interface area between metal and cement for both groups. The fluid test with coloured 0.9% saline solution injected into the medullary canal showed that there was a direct connection between the medullary canal and the implant under-surface. Both groups showed defects of the cement mantle that allowed lipid to penetrate the cement-metal interface, but group S showed significantly improved implant stability compared to group A. There was minor cement adhesion after the pull-out test with significantly decreased cement adhesion ratio for group A compared to group S. In addition, lipid contamination was observed on the underside of all prostheses after pull out.

Turgeon et al[39] investigated 30 patients in a clinical in vivo study using radiostereometric analysis (RSA) to determine the maximum total point motion (MTPM) for the Attune tibia component. The implantations of the components were performed using Palacos or Simplex cement and showed a mean MTPM of 160 µm (SD 70) after six months, 200 µm (SD 100) after one year, and 210 µm (SD 120) after two years. Compared to our in vitro measured relative motions under dynamic loading, the in vivo MTPM data were higher. For the Triathlon (Stryker, USA) prosthesis, one of the most commonly used prostheses according to the Australian registry,[40] Molt et al,[41] also using RSA, showed mean MTPM values of 460 µm (SD 290) at three months, 610 µm (SD 520) at one year, 650 µm (SD 660) at two years, and 660 µm (SD 380) at five years. Based on 21,000 evaluated tibial components, Pijls et al[3] showed that early migration and relative motion increase the risk of revision. Another type of failure mechanism that has been reported is tibial debonding, with detachment of cement from the metal under-surface of the implant.[4] Different causes for tibial debonding have been reported: Silva et al[8] found that the cementation of the stem has a significant influence. Contamination with blood or lipids could also lead to a significant decrease of the bond between metal and cement; Billi et al[23] reported that lipid contamination of the underside of the prosthesis could reduce the bond stability between implant and cement to almost zero. However, we could exclude lipid contamination during cement application to the prosthesis underside and to the bone/cement. After the pull-out test, we could observe fat contamination on the under-surface of all prostheses. Furthermore, similar to Billi et al,[23] we measured low maximum failure load, especially for the group without cement pockets. The cementation took place under ideal conditions, and a possible lipid contamination was checked during each individual cementation. Therefore, possible fat contaminations must have occurred during or after placement of the component. Bonutti et al[4] also reported, in relation to the Attune tibia component, an early aseptic loosening with failure of the cement-implant interface. In this context, missing cement pockets and fewer rotation-stabilizing components were blamed for the loosening of this prosthesis design. However, such failure mechanisms have also been observed in other prosthesis designs.[23,42,43]

One of the limitations of this study was the number of human leg pairs available to us. Another limiting factor was the cement timing. We only used optimal timing with early cement application, and a two-stage cementation technique. How implant stability behaves with single-stage cementing technique and later cement application needs to be investigated in further study. Furthermore, no other bone cements with different viscosities could be investigated. The investigated cement mantle defects could only be analyzed after the test to determine the maximum force. Therefore, there is a possible influence of the defects by the pull test. Although the selected loading scenario takes into account different extension and flexion angles, and the associated differences in shear stress on the tibial plateau, it was not possible to simulate physiological everyday loading in its entirety. The transferability of the results that additional cement pockets generally improve implant stability in an existing implant design cannot be determined. This should be checked individually for each implant design.

In conclusion, both tibial prosthesis designs showed cement mantle defects and a connection between bone/fat marrow and metal-cement interface. With regard to the Attune S+ component, the additional cement pockets showed a significantly reduced relative motion between implant and bone and a significantly increased maximum failure load. We attribute this enhanced implant stability of the tibial component to the additional cement pockets, which allow for improved mechanical cement adhesion. From a biomechanical point of view, this has further improved the fixation performance of the implant. However, the transferability of the experimental data to the patient should be confirmed by clinical studies.

References

1. **No authors listed**. Endoprothesenregister Deutschland - Jahresbericht 2019. EPRD Deutsche Endoprothesenregister gGmbH. 2019. https://www.eprd.de/fileadmin/user_upload/Jahresbericht_2019_doppelseite_2.0.pdf
2. **Kurtz S**, **Ong K**, **Lau E**, **Mowat F**, **Halpern M**. Projections of primary and revision hip and knee arthroplasty in the United States from 2005 to 2030. *J Bone Joint Surg Am.* 2007;89-A(4):780–785.
3. **Pijls BG**, **Valstar ER**, **Nouta K-A**, **et al**. Early migration of tibial components is associated with late revision. *Acta Orthop.* 2012;83(6):614–624.
4. **Bonutti PM**, **Khlopas A**, **Chughtai M**, **et al**. Unusually high rate of early failure of tibial component in ATTUNE total knee arthroplasty system at implant-cement nterface. *J Knee Surg.* 2017;30(5):435–439.

5. **Kutzner I**, **Hallan G**, **Høl PJ**, **et al**. Early aseptic loosening of a mobile-bearing total knee replacement. *Acta Orthop*. 2018;89(1):77–83.
6. **Pittman GT**, **Peters CL**, **Hines JL**, **Bachus KN**. Mechanical bond strength of the cement-tibial component interface in total knee arthroplasty. *J Arthroplasty*. 2006;21(6):883–888.
7. **Scott CEH**, **Biant LC**. The role of the design of tibial components and stems in knee replacement. *J Bone Joint Surg Br*. 2012;94-B(8):1009–1015.
8. **Silva M**, **Kabbash CA**, **Tiberi JV**, **et al**. Surface damage on open box posterior-stabilized polyethylene tibial inserts. *Clin Orthop Relat Res*. 2003;416(416):135–144.
9. **Cerquiglini A**, **Henckel J**, **Hothi H**, **et al**. Analysis of the Attune tibial tray backside: A comparative retrieval study. *Bone Joint Res*. 2019;8(3):136–145.
10. **Staats K**, **Wannmacher T**, **Weihs V**, **Koller U**, **Kubista B**, **Windhager R**. Modern cemented total knee arthroplasty design shows a higher incidence of radiolucent lines compared to its predecessor. *Knee Surg Sports Traumatol Arthrosc*. 2019;27(4):1148–1155.
11. **Lutz MJ**, **Halliday BR**. Survey of current cementing techniques in total knee replacement. *ANZ J Surg*. 2002;72(6):437–439.
12. **Phillips AM**, **Goddard NJ**, **Tomlinson JE**. Current techniques in total knee replacement: results of a national survey. *Ann R Coll Surg Engl*. 1996;78(6):515–520.
13. **Randall DJ**, **Anderson MB**, **Gililland JM**, **Peters CL**, **Pelt CE**. A potential need for surgeon consensus: Cementation techniques for total knee arthroplasty in orthopedic implant manufacturers' guidelines lack consistency. *J Orthop Surg*. 2019;27(3):230949901987825.
14. **Refsum AM**, **Nguyen UV**, **Gjertsen J-E**, **et al**. Cementing technique for primary knee arthroplasty: a scoping review. *Acta Orthop*. 2019;90(6):582–589.
15. **Galasso O**, **Jenny JY**, **Saragaglia D**, **Miehlke RK**. Full versus surface tibial baseplate cementation in total knee arthroplasty. *Orthopedics*. 2013;36(2):e151-8.
16. **Luring C**, **Perlick L**, **Trepte C**, **et al**. Micromotion in cemented rotating platform total knee arthroplasty: cemented tibial stem versus hybrid fixation. *Arch Orthop Trauma Surg*. 2006;126(1):45–48.
17. **Saari T**, **Li MG**, **Wood D**, **Nivbrant B**. Comparison of cementing techniques of the tibial component in total knee replacement. *Int Orthop*. 2009;33(5):1239–1242.
18. **Schlegel UJ**, **Bruckner T**, **Schneider M**, **Parsch D**, **Geiger F**, **Breusch SJ**. Surface or full cementation of the tibial component in total knee arthroplasty: a matched-pair analysis of mid- to long-term results. *Arch Orthop Trauma Surg*. 2015;135(5):703–708.
19. **Han HS**, **Lee MC**. Cementing technique affects the rate of femoral component loosening after high flexion total knee arthroplasty. *Knee*. 2017;24(6):1435–1441.
20. **Vaninbroukx M**, **Labey L**, **Innocenti B**, **Bellemans J**. Cementing the femoral component in total knee arthroplasty: which technique is the best? *Knee*. 2009;16(4):265–268.
21. **Vanlommel J**, **Luyckx JP**, **Labey L**, **Innocenti B**, **De Corte R**, **Bellemans J**. Cementing the tibial component in total knee arthroplasty: which technique is the best? *J Arthroplasty*. 2011;26(3):492–496.
22. **Wetzels T**, **van Erp J**, **Brouwer RW**, **Bulstra SK**, **van Raay JJAM**. Comparing cementing techniques in total knee arthroplasty: An in vitro study. *J Knee Surg*. 2019;32(9):886–890.
23. **Billi F**, **Kavanaugh A**, **Schmalzried H**, **Schmalzried TP**. Techniques for improving the initial strength of the tibial tray-cement interface bond. *Bone Joint J*. 2019;101-B(1_Supple_A):53–58.
24. **Franck H**, **Munz M**. Total body and regional bone mineral densitometry (BMD) and soft tissue measurements: correlations of BMD parameter to lumbar spine and hip. *Calcif Tissue Int*. 2000;67(2):111–115.
25. **Grupp TM**, **Holderied M**, **Pietschmann MF**, **et al**. Primary stability of unicompartmental knee arthroplasty under dynamic flexion movement in human femora. *Clinical Biomechanics*. 2017;41:39–47.
26. **Grupp TM**, **Pietschmann MF**, **Holderied M**, **et al**. Primary stability of unicompartmental knee arthroplasty under dynamic compression-shear loading in human tibiae. *Clinical Biomechanics*. 2013;28(9–10):1006–1013.
27. **Kutzner I**, **Bender A**, **Dymke J**, **Duda G**, **von Roth P**, **Bergmann G**. Mediolateral force distribution at the knee joint shifts across activities and is driven by tibiofemoral alignment. *Bone Joint J*. 2017;99-B(6):779–787.
28. **Kutzner I**, **Heinlein B**, **Graichen F**, **et al**. Loading of the knee joint during activities of daily living measured in vivo in five subjects. *J Biomech*. 2010;43(11):2164–2173.
29. **Clarius M**, **Seeger JB**, **Jaeger S**, **Mohr G**, **Bitsch RG**. The importance of pulsed lavage on interface temperature and ligament tension force in cemented unicompartmental knee arthroplasty. *Clinical Biomechanics*. 2012;27(4):372–376.
30. **Yushkevich PA**, **Piven J**, **Hazlett HC**, **et al**. User-guided 3D active contour segmentation of anatomical structures: significantly improved efficiency and reliability. *Neuroimage*. 2006;31(3):1116–1128.
31. **Faul F**, **Erdfelder E**, **Lang AG**, **Buchner A**. G*Power 3: a flexible statistical power analysis program for the social, behavioral, and biomedical sciences. *Behav Res Methods*. 2007;39(2):175–191.
32. **Schwarze M**, **Schonhoff M**, **Beckmann NA**, **Eckert JA**, **Bitsch RG**, **Jäger S**. Femoral cementation in knee arthroplasty-a comparison of three cementing techniques in a sawbone model using the ATTUNE knee. *J Knee Surg*. 2021;34(3):258–266.
33. **Sharkey PF**, **Lichstein PM**, **Shen C**, **Tokarski AT**, **Parvizi J**. Why are total knee arthroplasties failing today--has anything changed after 10 years? *J Arthroplasty*. 2014;29(9):1774–1778.
34. **Ries C**, **Heinichen M**, **Dietrich F**, **Jakubowitz E**, **Sobau C**, **Heisel C**. Short-keeled cemented tibial components show an increased risk for aseptic loosening. *Clin Orthop Relat Res*. 2013;471(3):1008–1013.
35. **Schlegel UJ**, **Püschel K**, **Morlock MM**, **Nagel K**. Effect of tibial tray design on cement morphology in total knee arthroplasty. *J Orthop Surg Res*. 2014;9:123.
36. **Schlegel UJ**, **Siewe J**, **Delank KS**, **et al**. Pulsed lavage improves fixation strength of cemented tibial components. *Int Orthop*. 2011;35(8):1165–1169.
37. **Jaeger S**, **Rieger JS**, **Bruckner T**, **Kretzer JP**, **Clarius M**, **Bitsch RG**. The protective effect of pulsed lavage against implant subsidence and micromotion for cemented tibial unicompartmental knee components: an experimental cadaver study. *J Arthroplasty*. 2014;29(4):727–732.
38. **Jaeger S**, **Eissler M**, **Schwarze M**, **Schonhoff M**, **Kretzer JP**, **Bitsch RG**. Early tibial loosening of the cemented ATTUNE knee arthroplasty - Just a question of design? *Knee*. 2021;30:170–175.
39. **Turgeon TR**, **Gascoyne TC**, **Laende EK**, **Dunbar MJ**, **Bohm ER**, **Richardson CG**. The assessment of the stability of the tibial component of a novel knee arthroplasty system using radiostereometric analysis. *Bone Joint J*. 2018;100-B(12):1579–1584.
40. **No authors listed**. Hip, Knee & Shoulder Arthroplasty: 2020 Annual Report. Australian Orthopaedic Association National Joint Replacement Registry (AOANJRR). 2020. https://aoanjrr.sahmri.com/annual-reports-2020 (date last accessed 3 March 2022).
41. **Molt M**, **Ryd L**, **Toksvig-Larsen S**. A randomized RSA study concentrating especially on continuous migration. *Acta Orthop*. 2016;87(3):262–267.
42. **Hazelwood KJ**, **O'Rourke M**, **Stamos VP**, **McMillan RD**, **Beigler D**, **Robb WJ**. Case series report: Early cement-implant interface fixation failure in total knee replacement. *Knee*. 2015;22(5):424–428.
43. **Kopinski JE**, **Aggarwal A**, **Nunley RM**, **Barrack RL**, **Nam D**. Failure at the tibial cement-implant interface with the use of high-viscosity cement in total knee arthroplasty. *J Arthroplasty*. 2016;31(11):2579–2582.

Author information:
- S. Jaeger, PhD, Deputy Director
- M. Schwarze, MD, Consultant, Orthopaedic Surgeon
- M. Schonhoff, M. Eng, Research Associate
- J. P. Kretzer, PhD, Director
  Laboratory of Biomechanics and Implant Research, Department of Orthopaedic Surgery, Heidelberg University Hospital, Heidelberg, Germany.
- M. Eissler, MD, Assistant Doctor for for Diagnostic and Interventional Radiology, Department of Diagnostic and Interventional Radiology, Heidelberg University Hospital, Heidelberg, Germany.
- R. G. Bitsch, MD, PhD, Orthopaedic Surgeon, Consultant, Laboratory of Biomechanics and Implant Research, Department of Orthopaedic Surgery, Heidelberg University Hospital, Heidelberg, Germany; ATOS Clinic Heidelberg, Heidelberg University, Heidelberg, Germany.

Author contributions:
- S. Jaeger: Conceptualization, Data curation, Methodology, Project administration, Writing – original draft, Writing – review & editing.
- M. Eissler: Formal analysis, Writing – review & editing.
- M. Schwarze: Data curation, Project administration, Writing – review & editing.
- M. Schonhoff: Data curation, Writing – review & editing.
- J. P. Kretzer: Conceptualization, Methodology, Writing – review & editing.
- R. G. Bitsch: Conceptualization, Writing original draft, Writing – review & editing.

Funding statement:
- The authors disclose receipt of the following financial or material support for the research, authorship, and/or publication of this article: the non-profit research fund of Stiftung Endoprothetik (Grant number S 01/18). No benefits in any form have been received or will be received from a commercial party related directly or indirectly to the subject of this article.

ICMJE COI statement:
- M. Schwarze reports receipt of equipment from Otto Bock Healthcare, and an institutional grant from Deutsche Arthrose-Hilfe e.V, unrelated to this study. P. Kretzer reports institutional grants from Johnson & Johnson DePuy, B. Braun Aesculap, DOT, Falcon Medical, Institut Straumann, Peter Brehm, Ceramtec, Implantcast, Mathys Orthopaedie, Permedia, Questmed, and SpineServe, all unrelated to this study. P. Kretzer also reports consulting payments from Ceramtec, speaker payments from Johnson & Johnson DePuy and Mathys, and receipt of equipment from Johnson & Johnson DePuy, Ceramtec, and Mathys Orthopaedie, all unrelated to this study. P. Kretzer holds an unpaid role as president of the Deutsche Gesellschaft für Bio-

mechanik. S. Jaeger reports institutional grants from Johnson & Johnson DePuy, B. Braun Aesculap, Waldemar Link, Heraeus Medical, Zimmer Biomet, Peter Brehm, Ceramtec, Implantcast, and Mathys Orthopaedie, unrelated to this study. S. Jaeger also reports receipt of equipment from Johnson & Johnson DePuy, Zimmer Biomet, Ceramtec, Mathys Orthopaedie, and Heraeus Medical, all unrelated to this study. R. G. Bitsch reports institutional grants from Johnson & Johnson DePuy, B. Braun Aesculap, Waldemar Link, Heraeus Medical, Zimmer Biomet, and Peter Brehm, all unrelated to this study, and speaker payments from Johnson & Johnson DePuy, also unrelated to this study.

Ethical review statement:
- The authors attained ethical approval for this study from the Institutional Review Board ID: S-351/2018.

Open access funding
- The authors confirm that the open access funding for this study was self-funded.